F2006V123

TRANSIENT PERFORMANCE OF A HYDRAULICALLY INTERCONNECTED SUSPENSION SYSTEM

Jeyakumaran, Jeku, Smith, Wade*, Zhang, Nong
University of Technology, Sydney, Australia.

ABSTRACT - This paper describes a vehicle dynamics model that captures the transient characteristics of a passive Hydraulically Interconnected Suspension (HIS) system. The vehicle is modeled as a lumped mass system with half-car and full-car configurations. Detailed fluid dynamics models are developed to represent the fluid nonlinearities and interactions between various hydraulic elements of the HIS. The developed models include pipelines, accumulators, nonlinear damper characteristics, and dynamics of actuating pistons and valves. Numerical integration of the second-order differential equations is carried out to evaluate the transient characteristics of the coupled mechanical and hydraulic systems. Vehicle performance and ride comfort are assessed from the time history of vertical displacements and accelerations when the vehicle moves over a bump profile. Simulation results show that the simplified half-car configuration captures the essential dynamics of the HIS system, however, it overestimates the vehicle displacements, accelerations and hydraulic pressure fluctuations. The developed simulation tools provide insight into various hydraulic design parameters and directions for design improvements relevant to HIS systems.

INTRODUCTION

The design of vehicle suspension systems involves a compromise between ride comfort and vehicle handling [1-3]. A softer suspension yields good ride performance with the expense of poor stability and directional control. Alternatively, a stiffer suspension enhances handling and minimizes the occurrence of vehicle rollover, yet it provides poor ride comfort. In recent decades, several suspension systems varying from passive to semi-active to fully active have been proposed to break the compromise between ride comfort and handling [4-7]. With the rapid development of sensing technologies, the recent trends are largely towards active, semi-active and slow-active suspension systems, and the superiority of these systems has been established in luxury passenger vehicles [8, 9]. In principle, active and semi-active suspension systems have the greatest capability to achieve optimum performance, however, the inherent drawbacks are the weight, cost, uncertain reliability, increased power consumption and complexity. Because of challenges associated with active controls with minimum hardware, the passive suspensions that enhance vehicle handling and stability are still of great interest for vehicle manufacturers.

Suspension researchers have paid attention to more effective passive systems that interconnect suspension actions between left and right, front and rear wheel-stations to provide optimal stiffness in bounce, pitch and roll motions. There are several interconnected vehicle suspensions acquainted in the automotive market [11, 12]. Published results show that the interconnected systems are very effective in reducing vehicle bounce, pitch or roll, as compared to independent suspension units. However, only limited systematic investigations

have been attempted on the dynamics of vehicles fitted with interconnected systems. In the mid 1990s, Rakheja et al. [12] and Liu et al. [13] applied fluid dynamics models for a Hydraulically Interconnected Suspension (HIS) system to predict vehicle stability and ride performance characteristics. However, complex fluid properties such as the nonlinear mechanical and fluid couplings, fluid inertia and wave propagation effects are not included in their mathematical models.

Recently, more novel HIS systems have been reported [14-17] and the superiority of these systems was demonstrated experimentally using the US National Highway Traffic Safety Administration's Fishhook Maneuver [17, 18]. Vehicle testing is used as the main tool for improving the HIS dynamic characteristics, however, this requires much effort and time during the product development process. Recently, the authors have developed a computationally efficient half-car model for the vibration analysis of a vehicle fitted with a HIS system [19, 20]. The most obvious limitation of that study was its linearity, i.e., the nonlinearities associated with the cylinder volume coupling, the accumulator air-spring effect, and damper valve characteristics were not included in the model formulation. In linear models, the parameters of the hydraulic oil are held constant, and therefore the pressure- and temperature-dependence of the fluid bulk modulus, viscosity and density are neglected. The coupling between mechanical and fluid systems, damper valve characteristics and variations in fluid properties are significant nonlinearities of the HIS and ride comfort evaluation requires accurate modelling of these nonlinearities.

In this paper, a mathematical model that captures the transient characteristics of a HIS is presented. The transient responses of the vehicle, measured by its roll, bounce and pitch motion, are investigated numerically using specified bump profiles. Simulation of the fluid exchanges/dynamics is carried out from the set of second-order differential equations describing the HIS system. In the next section, the description of the HIS system, model of the half-car and description of the hydraulic system model are presented. Then, simulation results are presented when a half-sine wave bump profile is specified to individual wheels.

MODEL DESCRIPTION

Mechanical System Model

The schematic diagram of a half-car model fitted with a HIS system is shown in Figure 1. The conventional shock absorbers and anti-roll bar assemblies between sprung vehicle body and unsprung wheel-stations are replaced with a HIS system. In a half-car model, the vehicle is represented with a lumped four-degree-of-freedom system. The model includes vehicle roll and bounce motions and vertical movements of two wheel-stations. The lateral and yaw motions of the vehicle are not included in the formulation. The stiffness and damping of the tires linked to the wheel-stations are included. The cylinder component is assumed as rigid in the horizontal directions. In a full-car model, the vehicle is
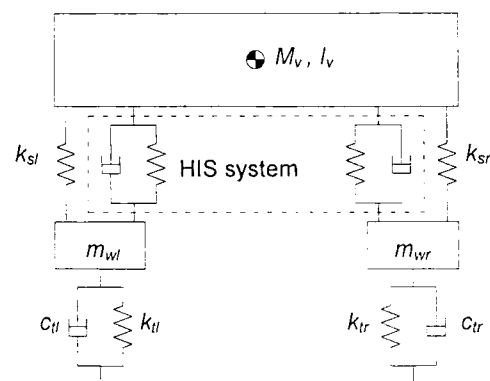

Figure 1: Schematic diagram of a typical half-car HIS system

modelled as a lumped system with seven-degrees-of-freedom to include vehicle pitch, roll, and bounce motions and vertical movements of four wheel-stations.

The equations of motion of the half-car mass and two wheel masses are derived from Newton's second law of motion. From the free body diagram of the half-car configuration, one can derive the equation of motion for the integrated system as:

$$[M]\{\ddot{Y}\} + [C]\{\dot{Y}\} + [K]\{Y\} = \{F\}$$

(1)

where $\{Y\}$, $\{\dot{Y}\}$, $\{\ddot{Y}\}$ and $\{F\}$ are the displacement, velocity, acceleration and force. The mass, damping and stiffness, $[M]$, $[C]$ and $[K]$ are 4 x 4 matrices with constant coefficients. The force vector, $\{F\}$, is dependent on the hydraulic system couplings and specified vertical rise/fall of the road profile to the individual wheels. The mechanical suspension is assumed linear and the tire is represented with a linear spring-damper combination.

Hydraulic System Model

The hydraulic schematic of the half-car HIS system is shown in Figure 2. This system replaces the conventional shock absorbers and anti-roll bar assemblies with interconnected hydraulic cylinders, accumulators, damper valves and fluid pipelines. The cylinders are kinetically linked to the two wheel-stations and the chassis. The hydraulic elements feature high fluid velocities, pressures and accelerations during fast transients and they are arranged such that vehicle bounce, pitch and roll motions operate with fluid flow through selected accumulators and dampers. The velocities and the forces applied to the pistons from the wheel-stations cause changes in the pressures and flow rates in the fluid circuits.
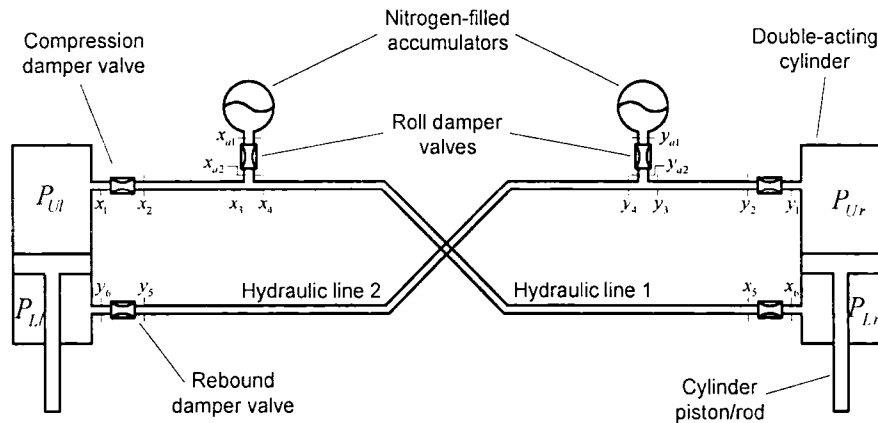

Figure 2: Hydraulic schematic diagram of a half-car HIS system

Accurate models are developed to represent the dynamics of pistons, damper valves and upper and lower cylinder chambers. The oil aeration is a significant nonlinearity in models of hydraulic circuits and it is an important parameter for the dynamic analysis. The fluid bulk modulus is modified to account for the air in the oil, and flexibility of hoses and pipelines. The differential equations that describe the pressure changes in terms of various system flow quantities can be written in the following generalized form

$$\dot{p} = \frac{\beta\ (p)}{V}\sum Q \ ; \qquad \beta\ (p) = \beta_0 + \beta_1 p$$

(2)

where $\dot{p}$ is the pressure rate, V is the fluid volume, $\beta(p)$ is the effective bulk modulus of the oil, and ΣQ represents the net flow to the fluid volume. The value $\beta(p)$ is described as a linear function of pressure with coefficients β_0 and β_1. The flow rates passing through the bleed holes, damper valves, flow restrictions in fluid lines and accumulators are described by standard turbulent orifice flow equations, i.e.,

$$Q = c_d \, A \, \sqrt{(p_1 - p_2)} \tag{3}$$

where Q is the flow rate through the orifice of area A, p_1 and p_2 are the pressure at ends 1 and 2, respectively, and c_d is the discharge coefficient. The pressure drop and flow resistance in the annular flows are dominated by the viscosity effect rather than the orifice flow, thus the pressure drop due to viscosity effects is also incorporated in the hydraulic system model.

The damper valves play an important role in the HIS system performance. The relationship between flow rate and pressure drop of the dampers is highly nonlinear, and simulation of such element requires modelling the interactions between fluid flow and cylinder-piston stroke. A typical valve characteristics is defined by the relationship between the volumetric flow rate and pressure difference. The valve characteristics are divided into three regions: a closed region, transient region and open region. During the steady state conditions, the valve is fully closed and flow is allowed through small bleed holes. During fast transients, the valve is fully open and the flow characteristics are determined from the valve dynamics and stiffness properties of the spring elements. In the transient region, the valve is partially open to avoid abrupt changes in flow and damping force. The equation of motion of the valves is primarily dictated by pressure forces, F_p, spring forces, F_s, damping forces, F_d, and flow forces, F_f, and can be written in the following generalized form

$$F_p + F_s + F_d + F_f = m \, \ddot{x}_s \tag{4}$$

where m is the piston/spool mass and, x and $\ddot{x}_s$ are the position and acceleration, respectively. For the half-car configuration, the equations of motion of four cylinder-damper valves, two accumulator valves and two cylinder-pistons are derived separately and coupled with the four-degree-of-freedom mechanical system model.

The vehicle layout and packaging constraints of the suspension system requires relatively long flexible pipelines. A lumped parameter model is developed by dividing the fluid pipelines into several elements. The fluid pipe of constant diameter is handled as one element. The mean pressure and mean flow in each element is assumed as an arithmetic mean of the pressure and flow rate at both ends of the pipe. The fluid flow in the pipe is assumed as one-dimensional compressible flow to accommodate the water hammer phenomenon. The HIS system features gas-pressurized hydraulic accumulators to reduce shock pressure loading due to system inputs. The accumulator consists of a pressure housing divided into two chambers by an elastometric bladder. One chamber is filled with gas and the other chamber filled with hydraulic fluid. The compressibility of the oil in the accumulator is neglected, as the oil stiffness is much greater than that of the nitrogen contained in the bladder. The adiabatic gas law is used for representing the accumulator pressure as a function of gas volume at a precharged pressure. Detailed derivations are not presented here because of space limitations.

The resulting equations of motion are highly nonlinear and therefore numerical integration is carried out to determine the system states. The simulation is performed with Advanced Continuous Simulation Language (ACSL) utilizing Runge-Kutta-Fehlberg fourth order integration with variable time steps. The various system parameters such as cylinder chamber

and accumulator pressures, pressure losses in the pipe lines, junctions and damper valves, flow demands to cylinder chamber, gas volume, etc., are calculated at each time step.

RESULTS AND DISCUSSION

The developed mathematical models of the HIS system are investigated with a typical speed bump on an otherwise smooth road profile. A half-sine wave bump profile with a peak height of 0.12 m and a base length of 2 m is used in the simulation. Figures 3-5 show results of the half-car model when the left wheel rides over the bump starting at t=0.1 sec. The vehicle is driven at a speed of 24 km/h, and therefore the left wheel is over the bump between t=0.1 sec and t=0.4 sec. Figure 3 shows the left wheel displacement (dash line), vehicle bounce at the centre of gravity of the sprung mass (dot line) and the vehicle roll angle (thick solid line). The maximum left wheel and vehicle bounce displacements are 0.12 m and 0.07 m, occurring at t=0.28 sec and t=0.45 sec, respectively. The maximum bounce lags that of the maximum left wheel displacement by 0.17 sec as the force is transferred to the sprung mass through the HIS system. Referring to the thick line in Figure 3, the maximum roll angle is about 0.1 rad (~5.7°), occurring t=0.3 sec, just after the left wheel is at the peak of the bump.
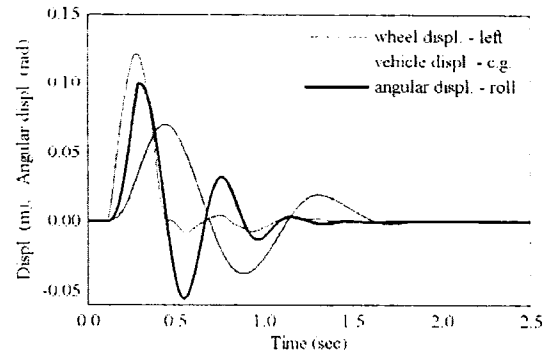

Figure 3: Wheel and bounce displacements: half-car model with bump on left wheel

Figure 4 shows the time history of wheel and vehicle bounce accelerations as the vehicle drives over the same bump at 24 km/h. The left wheel acceleration oscillates at the wheel hop frequency of about 11 Hz with a initial peak value of about 50 m/s^2, and it damps out quickly when the left wheel reaches the end of the bump at t=0.4 sec. The vehicle acceleration shows a peak value of only 3 m/s^2. To illustrate the significance of pressure characteristics, typical pressure traces of top-left cylinder, bottom-left cylinder and accumulator-1 are presented in Figure 5. For the system mean pressure of 20 bar, the maximum and minimum top-left chamber pressures are about 70 bar and 6.5 bar, respectively. As shown in Figure 2, the accumulator-1 is located in the hydraulic line-1 and linked to the top-left cylinder chamber, and therefore the pressure profiles of accumulator-1 closely resemble that of the top-left cylinder. Results also confirm that the
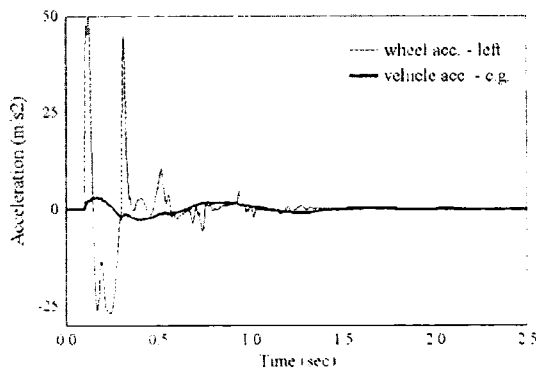

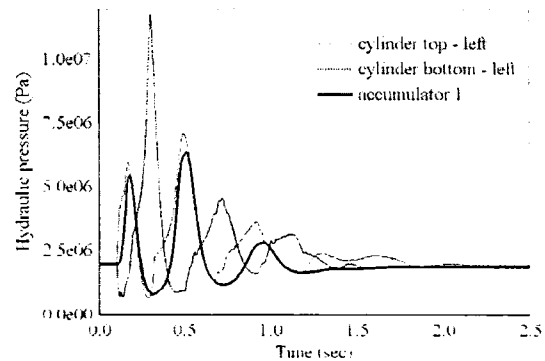Figure 4: Wheel and vehicle accelerations: half-car model with bump on left wheel

Figure 5: Typical hydraulic pressure profiles: half-car model with bump on left wheel

initial drop in the top-left cylinder pressure is accompanied by flow from accumulator-1 during typical vehicle roll motion. The cylinder chamber pressures continue to oscillate about the mean pressure of 20 bar, long after the left wheel reaches the end of the bump at t=0.4 sec.

Figures 6-10 show the results corresponding to the full-car model when the front- and back-left wheels ride over the same bump profile. These results simulate a vehicle with a wheel base of 3 m driven at a speed of 24 km/h. The front-left and back-left wheels start riding over the bump at t=0.10 sec and t=0.55 sec, respectively, and the right wheels are specified with zero vertical displacements. Figure 6 shows the front-left wheel displacement (dash line), back left-wheel displacement (dot line), vehicle bounce (thick solid line), and the vehicle roll displacement (thin solid line). The vehicle pitch displacement (thick solid line) together with the front-left wheel displacement (dash line) and back-left-wheel displacement (dot line) are also shown separately in Figure 7. The maximum front-left wheel and back-left wheel displacements are about 0.116 m and 0.125 m, occurring at t=0.28 sec and t=0.72 sec, respectively. The maximum pitch motion of about 2° occurs as the back-left wheel approaches the end of the bump at t=0.8 sec, and the oscillations damps out quickly at about t=2.0 sec. A comparison of results shown in Figures 3 and 6 indicates that the time history of wheel displacements are very similar, however, the half-car model overestimates the vehicle bounce and roll displacements. Referring to Figure 6, the maximum vehicle bounce displacement predicted by the full-car model is 0.035 m. This value is about 50% of the corresponding value predicted by the half-car model in Figure 6.
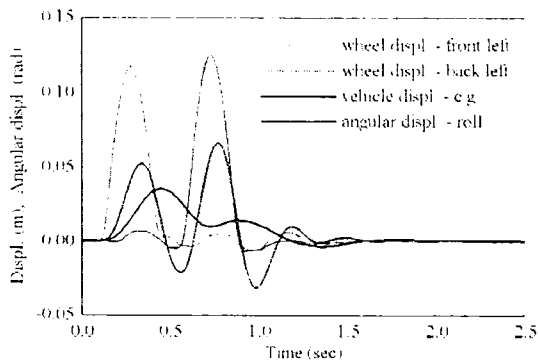

Figure 6: Wheel and vehicle displacements: full-car model with bump on left wheels
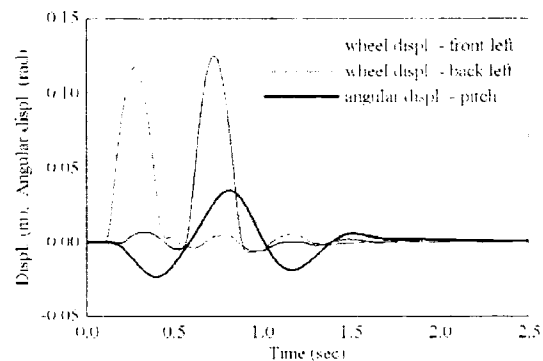

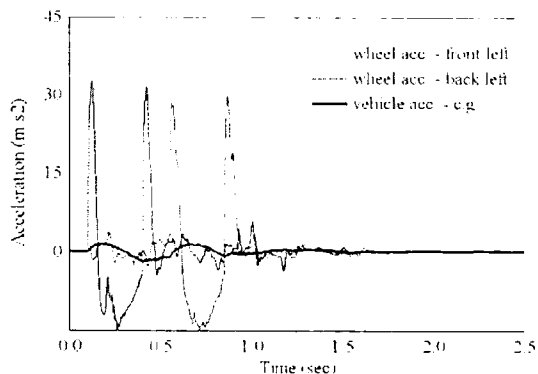Figure 7: Wheel and pitch displacements: full-car model with bump on left wheels

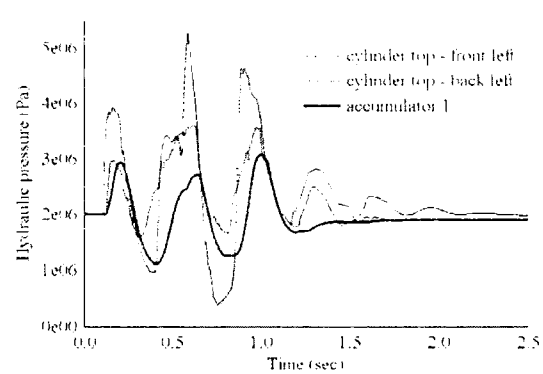Figure 8: Wheel and vehicle accelerations: full-car model with bump on left wheels

Figure 9: Typical hydraulic pressure profiles: full-car model with bump on left wheels

The front-left and back-left wheel accelerations and vehicle acceleration of the full-car model are presented in Figure 8. The time history of the acceleration traces shows very similar acceleration characteristics to the half-car results shown in Figure 4, however, the magnitudes of the wheel accelerations are again overestimated in the half-car configuration. The maximum left wheel acceleration is 32 m/s^2 where the half-car model predicts the value of 50 m/s^2. Figure 9 shows the typical pressure traces corresponding to the top-front-left cylinder and top-back-left cylinder chambers and accumulator-1. The top-front-left and top-back-left cylinder chamber pressures show very similar frequency components. The maximum and minimum top-front-left chamber pressures are about 40 bar and 10 bar, respectively. These pressure oscillations are much lower than the corresponding values of 70 bar and 6.5 bar reported with the half-car configuration.

Figure 10 shows the reaction forces on the front-left wheel (solid line) and back-left wheel (dot line) when the front- and back-left wheels ride over the bump profile. The reaction force at the front-left wheel increases rapidly due to the sudden change in road gradient when the front-left wheel hits the bump at t=0.1 sec, and reaches a maximum value of about 7.0 kN. Similarly, the reaction force at the back-left wheel increases rapidly when it hits the bump at t=0.55 sec, and reaches a maximum value of about 7.5 kN. The reaction force exerted by the road is upwards, and wheel lift-off over the bump occurs when the reaction becomes zero. The wheel lift-off event determines the upper limit of the vehicle speed without losing contact with the road. In Figure 10, the minimum reaction forces on the front-left wheel and back-left wheels are 800 N and 950 N, occurring at about t=0.4 sec and t=0.8 sec, respectively.
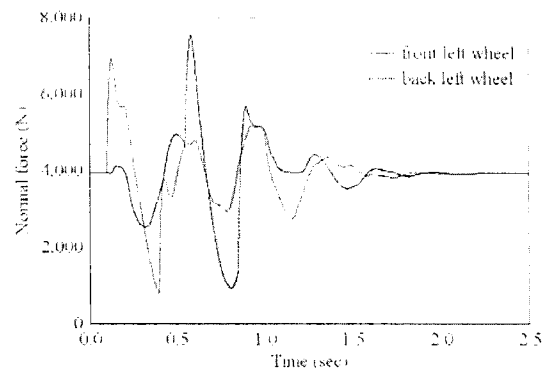

Figure 10: Wheel reaction forces: full-car model with bump on left wheels

Figures 11-14 show the simulation results from the full-car model when the vehicle is driven over the half-sine wave bump profile at a speed of 24 km/h. Both front wheels and both back wheels start riding over the bump at t=0.10 sec and t=0.55 sec, respectively. Figure 11 shows the front wheel displacement (dash line), back wheel displacement (dot line), vehicle bounce (thick solid line), and vehicle roll displacement (thin solid line). Because of the assumed left-right symmetry and the bump profile is specified to the left and right wheels, the time history
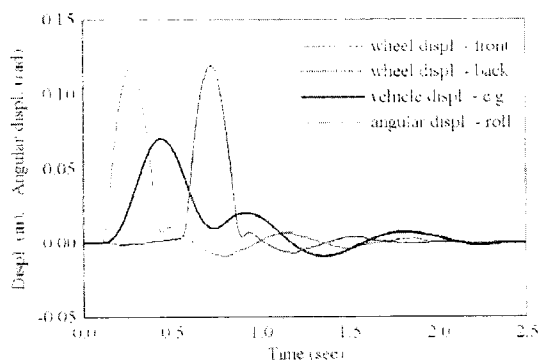

Figure 11: Wheel and vehicle displacements: full-car model with bump on all wheels
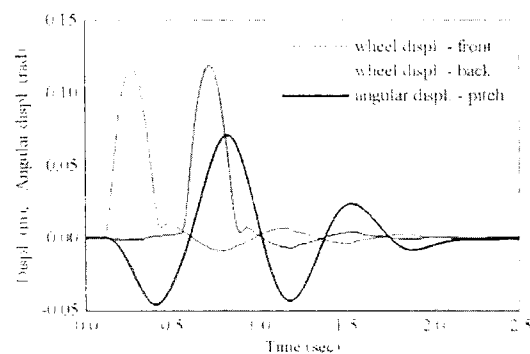

Figure 12: Wheel and vehicle displacements: full-car model with bump on all wheels

of the roll displacement is zero. Figure 12 shows the pitch displacement of the vehicle (thick solid line) together with the front-left wheel displacement (dash line) and back left-wheel displacement (dot line). The maximum front and back wheel displacements are about 0.117 m and 0.119 m, occurring at t=0.28 sec and t=0.72 sec, respectively. These wheel displacements are very similar to those presented in Figures 6 and 7. The front and back wheel accelerations and vehicle acceleration of the full-car model are presented in Figure 13. The time history of the acceleration traces shows similar acceleration characteristics as presented in Figure 8. The wheel accelerations oscillate at the wheel hop frequency with a
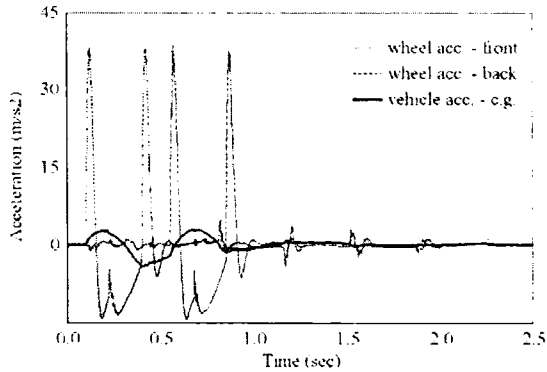

Figure 13: Wheel and vehicle accelerations: full-car model with bump on all wheels
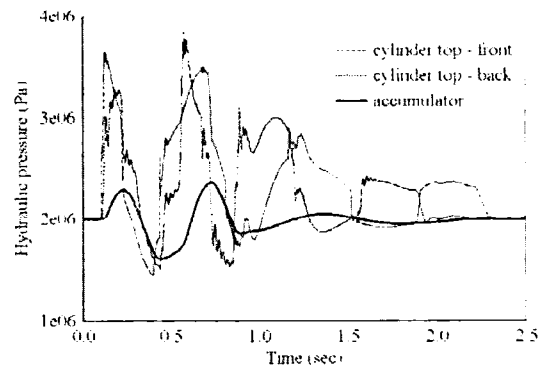
Figure 14: Typical hydraulic pressure profiles: full-car model with bump on all wheels

peak value of about 38 m/s^2. Figure 14 shows the typical pressure traces corresponding to the top-front cylinder and top-back cylinder chambers and accumulator-1. With the absence of the roll motion, the pressure oscillations in the cylinders and accumulators are significantly lower than the values presented in Figures 5 and 9.

CONCLUSIONS

A vehicle dynamic model that captures the transient characteristics of a HIS system is presented. The vehicle is modelled as a lumped mass system with a half-car model with four degrees of freedom and a full-car model with seven degrees of freedom. Mathematical models are developed to represent the nonlinearities associated with pressure-flow characteristics, fluid properties, damper valves, accumulators and coupling between mechanical and fluid systems. The vehicle ride performance is evaluated from the time history of vertical displacements and accelerations when the vehicle moves over a typical half-sine wave bump profile. Simulation results show that the simplified half-car configuration captures the essential dynamics of the HIS system, however, it overestimates the vehicle displacements, accelerations and hydraulic pressure fluctuations. The developed simulation model provides insight into various hydraulic system parameters and nonlinearities, and reveals directions for design improvements for vehicles fitted with HIS systems.

REFERENCES

1.   Mock, FC, "Relation of Spring-Suspension to Riding Qualities", SAE Technical Paper, No. 260045, 1926.
2.   Dillman, OD and Collier, EJ, "Building Stability into the Modern Automobile", SAE Technical Paper, No. 530036, 1953.

3. Gillespie, TD, "Fundamentals of Vehicle Dynamics", SAE International, Warrendale, Pa., 1992.
4. Sharp, RS and Crolla, DA, "Road Vehicle Suspension System Design - A Review", Vehicle System Dynamics, 16, pp. 167-192. 1987
5. Zapletal, E, "Balanced Suspension", SAE Technical Report, Proc. of the 2000 SAE Motorsports Engineering Conference & Exposition, 2000.
6. Smith, MC and Wang, FC, "Performance Benefits in Passive Vehicle Suspensions Employing Inerters", Proc. of the 42nd IEEE Conf. on Decision and Control, pp. 2258-2263, 2003.
7. Cooke, R, Crolla, DA and Abe, M, "Modelling Combined Ride and Handling Maneuvers for a Vehicle with Slow-active Suspension", Vehicle System Dynamics, 27, pp. 457-476, 1997.
8. Sims, ND and Stanway, R, "Semi-active Vehicle Suspension Using Smart Fluid Dampers: A Modelling and Control Study", International Journal of Vehicle Design, 33 (1-3), pp. 76-102, 2003.
9. Watton, J, Holford KM and Surawattanawan, P, "Electrohyraulic Effects on the Modelling of a Vehicle Active Suspension", Proc. IMechE., Part D: Journal of Automobile Engineering, 215 (6), pp. 1077-1092, 1991.
10. Ortiz, M, "Principles of Interconnected Suspension", Racecar Engineering, 7(7-8), 1997.
11. Mace, N, "Analysis and Synthesis of Passive Interconnected Vehicle Suspensions", PhD Thesis, University of Cambridge, 2004.
12. Rakheja, S, Liu, PJ, Ahmed, AKW and Su, H, "Analysis of an Interlinked Hydro-pneumatic Suspension", Advanced Automotive technologies, 52, pp. 279-287, 1993.
13. Liu, PJ, Rakheja, S and Ahmed AKW, "An Analytical Study of an Interconnected Vehicle Suspension", Advanced Automotive technologies, 56, pp. 151-160, 1995.
14. Heyring, CB, "Vehicle suspension system", United States Patent 5480188, 1996.
15. Fontdecaba, J, "Integral Suspension System for Motor Vehicles Based on Passive Components", SAE Technical Paper, No. 2002-01-3105, 2002.
16. Smith, MC and Walker, GW, "Interconnected Vehicle Suspension", Proc. IMechE., Part D: Journal of Automobile Engineering, 219 (3), pp. 295-307, 2005.
17. Wilde, JR, Heydinger, GJ, Guenther, DA, Mallin T, and Devenish, AM, "Experimental Evaluation of Fishhook Maneuver Performance of a Kinetic^{TM} Suspension System", SAE Technical Paper, No. 2005-01-0392, 2005.
18. Garrott, WR, Forkenbrock, GJ and Howe, JG, "Results from NHTSA's Experimental Examination of Selected Maneuvers that may Induce On-Road Untripped", Light Vehicle Rollover, SAE Technical Paper, No. 2001-01-0131, 2001.
19. Zhang, N, Smith, WA and Jeyakumaran, J, "Free Vibration of Vehicles with Hydraulically Interconnected Suspensions", in preparation, 2006.
20. Smith, WA, Zhang, N, and Jeyakumaran, J, "Ride Simulations of a Half-car with a Hydraulically Interconnected Passive Suspension", Submitted to FISITA-2006 World Automotive Congress, Japan, 2006.